

astroCAMP: A Community Benchmark and Co-Design Framework for Sustainable SKA-Scale Radio Imaging

Denisa-Andreea Constantinescu
 denisa.constantinescu@epfl.ch
 ESL, EPFL
 Lausanne, Switzerland

Etienne Orliac
 etienne.orliac@epfl.ch
 SCITAS, EPFL
 Lausanne, Switzerland

Hugo Miomandre
 hugo.miomandre@insa-rennes.fr
 Univ Rennes, INSA Rennes, CNRS,
 IETR - UMR 6164
 F-35000 Rennes, France

Rubén Rodríguez Álvarez
 ruben.rodriguezalvarez@epfl.ch
 ESL, EPFL
 Lausanne, Switzerland

Mickaël Dardaillon
 mickael.dardaillon@insa-rennes.fr
 Univ Rennes, INSA Rennes, CNRS,
 IETR - UMR 6164
 F-35000 Rennes, France

Miguel Peón-Quirós
 miguel.peon@epfl.ch
 EcoCloud, EPFL
 Lausanne, Switzerland

David Atienza
 david.atienza@epfl.ch
 ESL, EPFL
 Lausanne, Switzerland

Jacques Morin
 jacques.morin@insa-rennes.fr
 Univ Rennes, INSA Rennes, CNRS,
 IETR - UMR 6164
 F-35000 Rennes, France

Sunrise Wang
 sunrise.wang@oca.eu
 Univ Côte d'Azur, OCA, CNRS,
 J-L.Lagrange - UMR 7293
 F-06000 Nice, France

Jean-François Nezan
 jean-francois.nezan@insa-rennes.fr
 Univ Rennes, INSA Rennes, CNRS,
 IETR - UMR 6164
 F-35000 Rennes, France

metrics and thresholds to accelerate principled optimisation for SKA-scale imaging.

Keywords

radio astronomy, interferometric imaging, benchmarking, co-design, HPC, energy efficiency, carbon-aware computing, reproducibility

1 Introduction

Modern radio interferometers are entering a regime where *computing, not photon collection, limits scientific capability*. Arrays such as LOFAR, MWA, ASKAP, and the VLA already generate visibility, calibration, and imaging workloads that strain current HPC facilities, and these pressures intensify for the Square Kilometre Array (SKA), the most data-intensive radio observatory ever built. SKA-Low and SKA-Mid—illustrated in Fig. 1—will stream \sim 8–20 Tb/s of correlated visibilities to two Science Data Processors (SDPs), each expected to operate within a site-level power cap of 5 MW for several decades [6, 10]. Because both SDPs are located on carbon-intensive grids in South Africa and Australia, energy efficiency directly determines operational cost, scientific throughput, and long-term sustainability.

Efficiency requirements for SKA SDPs. Public SKA design documents [6, 10] indicate that the Science Data Processor (SDP) must sustain approximately 16–42 PFLOP/s for SKA-Low and 20–72 PFLOP/s for SKA-Mid, depending on observing mode. For a sustained compute requirement C_{sus} and power envelope P_{cap} , the facility-level efficiency is $\eta_{\text{facility}} = \frac{C_{\text{sus}}}{P_{\text{cap}}}$. Only a fraction of this

Abstract

The Square Kilometre Array (SKA) project will operate one of the world’s largest continuous scientific data systems, sustaining petascale imaging under strict power caps. Yet current radio-interferometric pipelines utilise only a small fraction of hardware peak performance—typically 4–14%—due to memory and I/O bottlenecks, resulting in poor energy efficiency and high operational and carbon costs. Progress is further limited by the absence of standardised metrics and fidelity tolerances, preventing principled hardware–software co-design and rigorous exploration of quality–efficiency trade-offs. We introduce astroCAMP, a framework for guiding the co-design of next-generation imaging pipelines and sustainable HPC architectures that maximise scientific return within SKA’s operational and environmental limits. astroCAMP provides: (1) a unified, extensible metric suite covering scientific fidelity, computational performance, sustainability, and lifecycle economics; (2) standardised SKA-representative datasets and reference outputs enabling reproducible benchmarking across CPUs, GPUs, and emerging accelerators; and (3) a multi-objective co-design formulation linking scientific-quality constraints to time-, energy-, carbon-to-solution, and total cost of ownership. We release datasets, benchmarking results, and a reproducibility kit, and evaluate co-design metrics for WSClean and IDG on an AMD EPYC 9334 processor and an NVIDIA H100 GPU. Further, we illustrate the use of astroCAMP for heterogeneous CPU–FPGA design-space exploration, and its potential to facilitate the identification of Pareto-optimal operating points for SKA-scale imaging deployments. Last, we make a call to the SKA community to define quantifiable fidelity

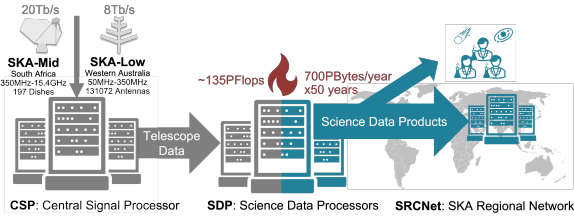


Figure 1: SKA’s infrastructure includes 2 Central Signal Processors (CSPs), 2 Science Data Processors (SDPs), and a global network of data centers (SRCNet). The SKA-Low and SKA-Mid telescopes will stream 28 Tb/s of data to the CSPs, and the SDPs will process it into science data products.

power is available to compute nodes, as modern HPC systems incur 30–40% overheads for networking, memory, storage, and cooling (PUE 1.3–1.4). Adopting $f_{\text{overhead}} \in [0.3, 0.4]$, the compute-node requirement becomes $\eta_{\text{compute}} = \frac{C_{\text{sus}}}{P_{\text{cap}}(1-f_{\text{overhead}})}$.

Fig. 2 summarizes the required energy efficiency ranges for SKA-Low and SKA-Mid under 1–5 MW power caps. A 2 MW allocation for SKA-Low and SKA-Mid requires tens of GFLOP/s/W, comparable to the average *Green500* systems in November 2025. These typically deliver 30–40 GFLOP/s/W. KAIROS, the current *Green500* leader, reaches 73.28 GFLOP/s/W [33]. This is comparable to the most computationally demanding operation case for SKA-Low, under a power cap of 1 MW. However, *Green500* benchmarking numbers reflect idealised, compute-bound kernels (LINPACK), whereas SKA imaging workloads are overwhelmingly memory- and I/O-limited (gridding, FFTs, deconvolution). Even with major algorithmic advances—such as w -projection [9], w -stacking [23], faceting, and IDG [34]—radio imaging remains dominated by memory bandwidth, data movement, and irregular access patterns.

The utilisation gap for imaging software deployments. On modern CPU and GPUs, imaging pipelines typically sustain only 4–14 % of peak floating-point performance [36], revealing a fundamental mismatch between imaging workloads and commodity architectures. This utilization inefficiency can be appreciated by comparing the required SKA-Low and Mid performance with the pink band in Fig. 2. Earlier modelling [6] reported only 10–20% efficiency for FFT- and gridding-dominated workloads, indicating that *naively scaling* existing pipelines to SKA data rates would demand tens of megawatts—far beyond the SDP site power caps. This gap has direct implications for both the feasibility and long-term sustainability of the SKA. Without substantial improvements in software efficiency and hardware utilisation, meeting SKA’s scientific throughput requirements would necessitate excessive overprovisioning of compute infrastructure and inevitably exceed the power budget. The underlying issue is that bandwidth-bound kernels draw significant power even when compute units remain under-utilised, leading to high operational and carbon costs for comparatively little scientific return.

Closing this gap requires more than incremental optimization of hardware and software tuning. It demands holistic co-design across algorithms, data structures, and hardware:

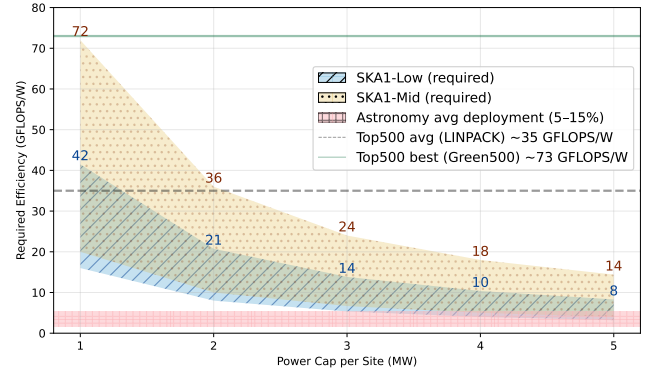


Figure 2: Required energy efficiency for the SKA-Low and SKA-Mid SDPs across 1MW to 5MW site power caps (orange and blue). Solid line: *Green500* best-in-class efficiency. Dashed line: average Top500 efficiency. The pink band shows the “astronomy average deployment”.

- (1) **Algorithmic optimisation:** reduce data movement through hierarchical memory reuse, structured sparsity, and compressed visibility formats.
- (2) **Domain-specific accelerators:** exploit GPUs, FPGAs, custom architectures, and ASICs optimised for imaging hotspots.
- (3) **Energy-aware orchestration:** use dynamic power scaling and locality-aware scheduling to match data-access patterns.

Enabling principled co-design further requires (1) standardised reference datasets; (2) cross-layer metrics integrating performance, energy, carbon, and cost; (3) science-driven image-quality tolerances; and (4) a reproducible framework for evaluating algorithms and systems under realistic SKA constraints. The community lacks such an infrastructure, obscuring the central question for SKA-scale computing: *how much scientific fidelity can be traded for performance, energy, and carbon savings without compromising discovery?* Other fields have solved similar challenges. Machine learning, for example, overcame a similar lack of standardisation through community benchmarks such as MLPerf [12, 24], unified datasets, accuracy thresholds, and submission protocols. Radio astronomy lacks an equivalent effort. These gaps hinder agile innovation in the domain and prevent researchers and developers from comparing Fig.s of merit without re-running large, expensive experiments.

Scope and contributions of this work. Towards bridging these gaps, this paper introduces **astroCAMP**, a reproducible benchmarking and co-design framework for radio-interferometric imaging. **astroCAMP** provides the metrics, datasets, and benchmark cases required to evaluate efficiency, sustainability, and quality trade-offs across high-performance and heterogeneous architectures. The contributions are:

- (1) **A unified cross-layer metric suite.** We define and implement a set of 12+ measurable metrics spanning performance, energy, carbon, system behaviour, economic cost, and scientific fidelity, providing a consistent basis for comparing imaging pipelines across CPUs, GPUs, FPGAs, ASICs, and emerging accelerators.

(2) **Standardised SKA benchmark suite and datasets.** We provide visibility datasets, reference dirty images, and parameterised benchmark configurations in the astroCAMP GitHub repository [27]. With this, we aim to enable reproducible, cross-platform evaluation of SKA imaging pipelines and systematic exploration of hardware–algorithm co-design trade-offs.

(3) **A multi-objective co-design formulation.** We formalise imaging as an optimisation problem over algorithmic and architectural parameters, with objectives such as time-to-solution, energy-to-solution, and carbon-to-solution under explicit quality, cost, and power constraints.

(4) **A reproducible design-space exploration workflow.** Using the PREESM framework [30], we demonstrate for a subset of astroCAMP’s metrics suite how astroCAMP can enable multi-objective design-space exploration and the computation of Pareto fronts in the metrics domain space.

Together, the four contributions form the foundation of the first end-to-end methodology for rigorously evaluating and co-designing SKA-scale imaging pipelines with carbon and cost efficiency as first-class objectives.

The remainder of this paper is organized as follows. Section 2 outlines the sustainability goals and challenges of the SKA SDP. Section 3 presents the astroCAMP framework and co-design methodology. Section 4 introduces the multi-objective co-design formulation and Section 5 the benchmark suite. Section 6 reports the experimental evaluation and results, while Section 7 discusses their implications for hardware–software co-design. Section 8 concludes the paper.

2 SKA SDP Sustainability Challenges and Gaps

Why does optimizing efficiency matter? Recent studies highlight the ecological impact of large-scale scientific computing in astronomy [3, 11, 16, 22]. In response, the SKA Observatory has embedded **sustainability and net-zero objectives** into its 50-year roadmap, aligned with the *UN Sustainable Development Goals*, and adopted the CO₂ Performance Ladder to support its net-zero transition [28, 29].

For the SDPs, the challenge is not only sustaining near-real-time throughput but doing so *efficiently*. Both sites operate on comparatively carbon-intensive grids based on the last twelve months of ElectricityMaps [1]: 0.672 kg CO₂/kWh in South Africa (SA) and 0.321 kg CO₂/kWh in Western Australia (WA). Continuous 1 MW to 5 MW operation therefore emits 5.9 kt CO₂/yr to 29.5 kt CO₂/yr (SA) and 2.8 kt CO₂/yr to 14.1 kt CO₂/yr (WA), excluding embodied carbon. **This makes computational efficiency a direct lever on SKA SDPs’ environmental footprint.**

Because operational emissions scale directly with compute efficiency, the limitations of current platforms become critical. In practice, low arithmetic intensity and utilisation mean:

- **Scalability failures:** bandwidth-bound kernels cannot strongly scale across many CPU/GPU nodes, limiting throughput even as hardware is added.
- **Higher operational and capital costs:** more nodes are required to offset low utilisation, increasing electricity and cooling demands.
- **Higher carbon emissions:** fewer images, catalogues, and time series are delivered per ton of CO₂ emitted.

Energy efficiency, utilisation, and parallel scaling are therefore not just performance metrics but **climate performance indicators**, coupling algorithmic design and hardware co-design to measurable carbon reduction. A factor-of-two improvement in application-level GFLOP/s/W directly halves SDP operational emissions at fixed science throughput. Moreover, utilization improvement reduces total cost of ownership by lowering both CAPEX and OPEX [2].

2.1 Gaps in Current Evaluation Practice

Table 1: Metric coverage across imaging tools: pipelines (WS-Clean, DDFacet, BIPP, WS-Snapshot), algorithmic kernels (IDG), and hardware kernels (FPGA-RP). Symbols: explicit (✓), implicit (~), missing (–). Metrics are detailed in Table 2.

Metric Category	WSClean	IDG	DDFacet	FPGA	BIPP	WS-S.	This
Pub. Year	2014	2018	2020/23	2022	2025	2025	–
System-level (heterogeneous node / pipeline)							
A1 Time-to-solution T_c	✓	✓	✓	✓	✓	✓	✓
A2 Energy-to-solution E_c	–	~	–	✓	–	–	✓
A3 Throughput Θ (vis/s)	✓	✓	~	✓	✓	~	✓
A4 Energy efficiency η_E	–	~	–	✓	–	–	✓
Hardware platform-level (CPU / GPU / FPGA / ASIC)							
A5 Utilisation / occupancy U	–	~	–	✓	–	–	✓
A6 Memory bandwidth B_{mem}	–	✓	–	✓	–	–	✓
A7 Peak memory usage M_{peak}	~	~	~	~	~	✓	✓
Sustainability							
C1 Carbon-to-solution C_c	–	–	–	–	–	–	✓
C2 Carbon efficiency η_C	–	–	–	–	–	–	✓
Economics							
E3 Cost efficiency	–	–	–	–	–	–	✓

Recent wide-field imaging studies have delivered significant advances in algorithmic sophistication and numerical fidelity, yet their evaluation methodology remains largely *performance-centric*. As summarised in Table 1, runtime and dirty-image RMS are consistently reported across WSClean [21], BIPP [32], WS-Snapshot [37], IDG [34], FPGA-RP [8], and DDFacet [18, 31], but key architecture-level metrics—power, energy-to-solution, energy efficiency, roofline characterisation, bandwidth sensitivity, and hardware utilisation—are either missing or only implicitly analysed. Even in DDFacet, where multi-node parallelisation has been demonstrated [18], no measurements of power or energy per job are reported. This limits and slows quantitative comparison across CPUs, GPUs, FPGAs, and emerging accelerators towards optimizing efficiency metrics.

System-level behaviour exhibits similar fragmentation. Pipeline-stage breakdowns and parallel efficiency are available in DDFacet’s distributed implementation [18], and partially in IDG [34] and FPGA-RP [8], but metrics such as device occupancy, data locality, bandwidth limits, and end-to-end dataflow behaviour are rarely treated systematically. This hinders the identification of system bottlenecks that directly influence scalability and energy efficiency in SKA-scale deployments.

None of the surveyed works reports carbon-to-solution, carbon efficiency, or any economic metrics, despite their increasing relevance given SKA’s strict power and environmental constraints. Overall, the literature reveals a fragmented evaluation landscape in which no existing study jointly assesses architecture-level

efficiency, system-level behaviour, algorithmic fidelity, and sustainability. To date, only one imaging study has reported total energy-to-solution [8], but only at the algorithmic kernel level (IDG), not for the entire imaging pipeline (WSClean). **astroCAMP** addresses this gap by providing a unified, reproducible, and cross-layer metric framework that enables principled algorithm–hardware co-design and supports energy-, carbon-, and fidelity-aware optimisation for large-scale imaging systems.

3 astroCAMP Framework

astroCAMP provides the missing infrastructure for reproducible, cross-layer evaluation of radio-interferometric imaging software and hardware. It unifies algorithmic, architectural, and sustainability metrics into a single benchmarking and co-design workflow (Fig. 3), enabling transparent comparison of imaging algorithms and hardware platforms. The framework enables designers to examine:

- (1) how algorithmic parameters (precision, kernel sizes, tiling) interact with CPU/GPU/FPGA platforms, supporting Outcome 1 by producing reusable, cross-platform performance and fidelity baselines;
- (2) which configurations satisfy SKA SDP power and throughput limits and populate Pareto-optimal performance–energy–quality trade spaces, delivering Outcome 2; and
- (3) how close commodity hardware can approach SKA efficiency targets and where accelerators are justified, directly informing Outcome 3 on energy- and carbon-efficient co-design.

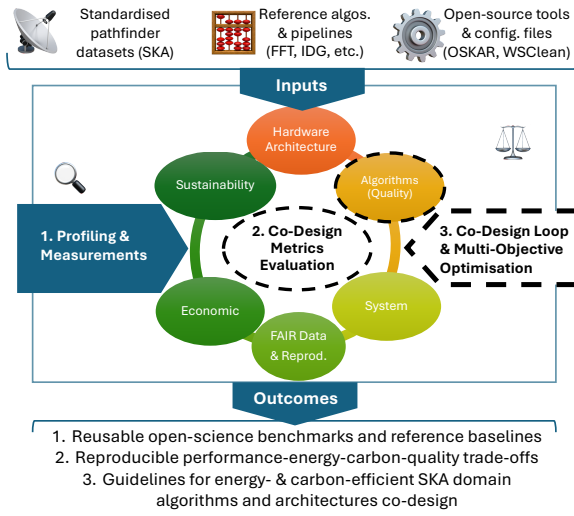


Figure 3: astroCAMP co-design framework. Dotted modules are intended for community extension.

3.1 Benchmarking and Co-Design Methodology

astroCAMP provides a reproducible methodology for evaluating radio-interferometric imaging pipelines across heterogeneous architectures. The framework standardises benchmark cases, input–output configurations, and a cross-layer metric suite (performance, energy, carbon, utilisation, and scientific fidelity), enabling fair

comparison of algorithmic variants and hardware platforms under realistic SKA-class constraints. The proposed methodology ensures that results obtained on different systems and with different imaging algorithms remain directly comparable. It consists of three non-overlapping stages (illustrated in Fig. 3):

1. Profiling & Measurements. Each benchmark is executed under controlled and repeatable conditions. We stabilise system behaviour (e.g., process pinning, NUMA placement, fixed-frequency modes when available) and begin runs only after the node reaches a steady thermal and power state. Experiments are repeated until runtime variance falls below a documented threshold. Rack-level power distribution units (PDUs) provide energy measurements to calculate energy-to-solution E_c , while platform telemetry (e.g., PMT [7] for CPUs, NVML for GPUs) is timestamp-aligned with PDU traces to validate device-level behaviour. From these measurements we derive time-to-solution T_c , throughput, and carbon-to-solution C_c using region-specific carbon intensity. All scripts, configurations, and reproducibility guidelines are openly available [27].

2. Co-Design Metrics Evaluation. For each benchmark configuration—including algorithmic parameters (e.g., IDG kernel sizes) and platform choice (CPU, GPU, FPGA)—we assemble a consistent vector of cross-layer metrics defined in Section 3.2. These metrics capture performance, energy, cost, sustainability, and system constraints (e.g., SKA SDP node power caps). This stage performs *metric computation only*: it normalises and validates measurements across systems, preparing a unified metric vector that serves as input to optimisation. In the current release, system and platform metrics are evaluated using PREESM [30], and sustainability/economic metrics via CEO-DC [2]. Algorithm-level quality metrics are intentionally excluded in this release and form an open call for the community to converge on standardised tolerances.

3. Co-Design Loop & Multi-Objective Optimisation. The metric vectors from Stage 2 feed into a structured design-space exploration (DSE) loop following the formulation in Section 4. The objective is to systematically evaluate alternative algorithm–architecture mappings and solve the resulting multi-objective optimisation problem to produce reproducible Pareto frontiers and trade-off curves. This stage provides the *interpretation layer*: identifying efficient regions of the design space, exposing performance–energy–quality bottlenecks, and determining when approximate methods or domain-specific accelerators become necessary to meet SKA-scale efficiency targets.

3.2 Co-design Metrics

astroCAMP includes a compact, cross-layer metric suite that links hardware behaviour, energy use, economic cost, and scientific fidelity. The framework measures hardware architecture (platform) and system performance using time-to-solution T_c , energy-to-solution E_c , average power, sustained memory bandwidth, utilisation, and domain-specific throughput (visibilities/s or images/s). Algorithmic quality is quantified via dirty-image RMS, PSNR/SIM, dynamic range, and astrometric and photometric errors from catalogue comparisons, capturing the scientific impact of approximations such as reduced precision, coarse w -stacking, or NUFFT kernel truncation. Sustainability metrics pair energy use with regional carbon intensity $\kappa(t, r)$ to compute Carbon-to-solution C_c ,

Table 2: astroCAMP co-design metrics. Core metrics (C) enter the performance–energy–quality optimisation; diagnostic metrics (D) support interpretation and reproducibility. Type symbols: Direct = •, Derived = ○, Proxy/Model-based = △.

Layer	ID	Metric / Formula	Unit	Role	Type	Instrumentation	Interpretation
System (Pipeline)	A1	Time-to-solution T_c	s	C	•	POSIX time, workflow logs, scheduler timestamps	End-to-end wall-clock runtime of the workload on the full (possibly heterogeneous) system, where T_c is the elapsed execution time.
	A2	Energy-to-solution $E_c = \int_0^{T_c} P(t) dt$	J	C	•	Rack/node PDUs, CPU RAPL, GPU NVML, PMT traces	Total electrical energy consumed by the system, integrating instantaneous power $P(t)$ over runtime T_c .
	A3	Throughput $\Theta = N/T_c$	vis/s	C	○	MS/FITS logs, visibility/image counters	System-level processing rate, where N is the number of visibilities or images processed during runtime T_c .
	A4	Energy efficiency $\eta_E = N/E_c$	vis/J	C	○	Derived from N and E_c	System-level science throughput per joule, using processed data volume N and energy-to-solution E_c .
Hardware Platform	A5	Utilisation $U = t_{\text{active}}/t_{\text{total}}$	–	C	•	nvidia-smi, ROCm tools, perf, Prometheus exporters	Fraction of time a device (CPU socket, GPU, FPGA, etc.) is actively running kernels, where t_{active} is active compute time and t_{total} is total wall time.
	A6	Memory bandwidth $B_{\text{mem}} = \text{Bytes}/T_c$	GB/s	D	•	Hardware counters, Intel VTune, NVIDIA Nsight	Sustained data-movement rate per platform, with B_{mem} indicating whether kernels are memory-bound.
	A7	Peak memory usage M_{peak}	GB	C	•	/proc/meminfo, nvidia-smi, cgroups, container telemetry	Maximum resident memory footprint observed on a platform during execution, constraining batch size and problem scaling.
Algorithmic Quality	B1	Dirty-image RMS $\sigma_{\text{dirty}} = \sqrt{\frac{1}{N} \sum (I_i - \bar{I})^2}$	Jy/beam	C	•	CASA/WSClean imstat, PyBDSF	Noise and artefact level in the dirty image, using pixel intensities I_i , mean value \bar{I} , and resulting RMS σ_{dirty} .
	B2	PSNR / SSIM $\text{PSNR} = 10 \log_{10} (I_{\text{max}}^2 / \text{MSE})$	dB / –	C	•	scikit-image, OpenCV	Fidelity of reconstruction \hat{I} vs. reference I_{ref} , using maximum pixel I_{max} and mean-squared error; SSIM measures structural similarity between \hat{I} and I_{ref} .
	B3	Dynamic range $DR = I_{\text{max}}/\sigma_{\text{res}}$	–	C	•	Residual-image statistics	Ratio of peak intensity I_{max} to residual RMS σ_{res} , determining detectability of faint emission.
	B4	Astrometric error $\epsilon_{\text{astro}} = \frac{1}{N} \sum \ x_i - x_i^{\text{ref}}\ $	arcsec or px	C	•	PyBDSF catalogues	Average positional discrepancy between reconstructed and reference sources, where x_i and x_i^{ref} are measured and reference positions.
Sustain.	C1	Carbon-to-solution $C_c = E_c \kappa(t, r)$	gCO ₂ e	C	△	Grid carbon-intensity APIs (e.g. electricityMap) + E_c	Total carbon footprint of a run, using measured energy E_c and grid carbon intensity $\kappa(t, r)$ at time t and region r .
	C2	Carbon efficiency $\eta_C = N/C_c$	vis/gCO ₂ e	D	○	Derived from N and C_c	Visibilities processed per gram CO ₂ emitted, normalising science throughput N by carbon cost C_c .
Economic	E1	Total cost ownership $C_{\text{TTO}} = C_{\text{capex}} + C_{\text{opex}}$	€	D	•	Procurement & operations records	Lifetime system cost, combining capital cost C_{capex} and operational cost C_{opex} .
	E2	Cost per job $C_E = E_c p_E$	€	C	○	Electricity tariff + E_c	Monetary cost per workload, using energy-to-solution E_c and electricity price p_E .
	E3	Cost efficiency Θ/C_{TTO}	vis/\$	D	○	Throughput + TTO data	Operations delivered per euro invested, using throughput Θ and total cost C_{TTO} .

enabling joint optimisation of energy, carbon, and image fidelity. Economic metrics—including cost per job $C_E = E_c p_E$ and amortised total cost of ownership C_{TTO} —connect computational choices to financial constraints relevant for large-scale SKA deployments.

Together, the full metric suite supports transparent, multi-objective co-design across CPU, GPU, FPGA, and ASIC platforms. Table 2 summarises all metrics, including their formulas, units, and instrumentation sources.

4 Extensible Multi-Objective Co-Design Formulation

astroCAMP provides a *general and extensible* co-design formulation that unifies algorithmic, architectural, and system-level degrees of freedom. Rather than prescribing specific algorithms or hardware, astroCAMP defines a *stable metric backbone* (Table 2) onto which current and future imaging algorithms (e.g., WSClean, IDG, BIPP), accelerator technologies (CPUs, GPUs, FPGAs, ASICs), and workflow runtimes can be instantiated.

Design space. Any imaging configuration is represented as a design point $x = (a, h, s) \in \mathcal{X}$, shown in Fig. 4, where:

- a are *algorithmic parameters*: precision, convolution kernel size, NUFFT or w -stacking order, snapshot parameters, visibility tiling, task fusion.
- h are *hardware parameters*: processor type, accelerator count, memory hierarchy, power caps, thread/block geometry.

- s are *system/workflow parameters* for mapping a to h : parallel decomposition, data-locality strategy, I/O staging, buffering and batching, workflow orchestration.

On the left side of Fig. 4, we see how each configuration x is evaluated on a fixed workload w (e.g. an SKA-Low or SKA-Mid benchmark) and is represented as a point in the design space of algorithmic, hardware platforms, and system parameters.

Metrics. For the DSE with astroCAMP framework, shown in Fig. 4, we consider the following core metrics detailed in Table 2:

$$T_c(x), E_c(x), C_c(x), \Theta(x), C_{\text{TTO}}, Q(x).$$

Here, T_c is time-to-solution, E_c is Energy-to-solution, C_c is Carbon-to-solution, Θ is throughput (e.g., visibilities/s or pixels/Joule), C_{TTO}

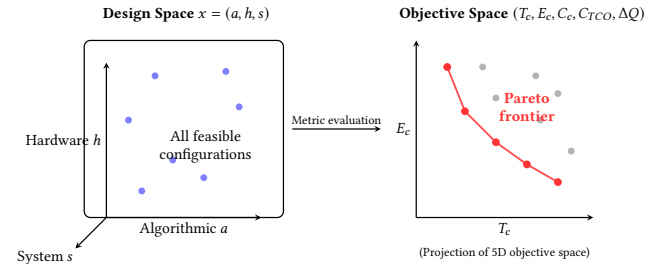


Figure 4: Overview of the astroCAMP co-design formulation.

is the total cost of ownership, and $Q(x)$ is a quality tuple (e.g., dirty-image RMS noise, PSNR). A high-fidelity reference configuration defines Q_{ref} . We measure scalarised quality loss as:

$$\Delta Q(x) = d(Q_{\text{ref}}, Q(x)),$$

where d is a weighted distance in quality space.

Multi-objective optimisation problem. We formalise co-design as a multi-objective optimisation problem subject to scientific and operational constraints.

$$\min_{x \in \mathcal{X}} (T_c(x), E_c(x), C_c(x), \Delta Q(x)) \quad (1)$$

Scientific quality constraint:

$$\Delta Q(x) \leq \Delta Q_{\text{max}}.$$

SDP operational constraints:

$$P_{\text{avg}}(x) \leq P_{\text{max}} \quad (\text{site power cap, e.g. 2 MW}), \quad (2)$$

$$\Theta(x) \geq \Theta_{\text{min}} \quad (\text{minimum throughput / survey cadence}), \quad (3)$$

$$x \in \mathcal{X}_{\text{valid}} \quad (\text{resource bounds, feasibility}). \quad (4)$$

Constraints couple algorithmic, hardware, and workflow choices to architectural, sustainability, and economic layers through energy, power, and carbon metrics. The formulation is modular: new algorithmic parameters extend a , new hardware platforms extend h , and new workflow or runtime options extend s . Additional metrics can be added to the objective or constraints without changing the optimisation structure. In this way, astroCAMP defines a *stable design space schema* that still accommodates future algorithmic and architectural innovation.

Because the objectives in Eq. (1) conflict, *no single optimal configuration exists*. We therefore compute the *Pareto frontier*

$$\mathcal{P} = \left\{ x \in \mathcal{X}_{\text{valid}} \mid x \text{ is not dominated across } (T_c, E_c, C_c, \Delta Q) \right\},$$

where “not dominated” means that there is no $x' \in \mathcal{X}_{\text{valid}}$ such that $T_c(x') \leq T_c(x), E_c(x') \leq E_c(x), C_c(x') \leq C_c(x), \Delta Q(x') \leq \Delta Q(x)$, with at least one inequality strict.

Each $x \in \mathcal{P}$ represents a distinct, scientifically valid, and operationally feasible trade-off (e.g., “fast but power-hungry”, “high precision but slower”, “energy-efficient but low throughput”). The construction of \mathcal{P} is done via structured parameter sweeps at the software and/or the hardware architecture level. Evaluation of co-design metrics can be performed using simulation tools [25], model-based design [30] or surrogate models. Automated design space exploration [38] can rely on Bayesian optimization [13], or evolutionary search to analyze how both new (BIPP, WS-Snapshot) and legacy algorithms (IDG) populate the multi-metric design space.

5 astroCAMP Benchmark Suite and Datasets

The benchmarks and datasets are designed to be large enough to stress memory, I/O, and communication layers while remaining manageable for design-space exploration experiments. We provide open, standardised benchmark cases, representative of radio-interferometric imaging workloads. Each case includes:

- Synthetic and pathfinder datasets derived from realistic telescope configurations (e.g. SKA-Low), generated with OSKAR;
- Reference outputs from validated CPU implementations (e.g. WSClean, IDG);

- Configuration files specifying baseline distribution, frequency range, integration time, and field of view.

The datasets were generated using OSKAR [19] (version OSKAR-2.11.2-dev 2025-07-17 ddb65ed) using SKA-Low 512 stations full configuration. Sixteen datasets were produced varying the number of timesteps (or time samples) over 1, 8, 64, 128, and 256, and the number of channels over 1, 8, 64, 128, and 256. Each timestep is integrated over 10 seconds. Phase center was set to 25.0 and -30.0 degrees in right ascension and declination, respectively. Start frequency was set to 151 MHz with increments of 1 MHz. Sources were selected from the GLEAM catalog [15] to cover a field of view of 40 degrees. Data volumes range from megabytes to terabytes, enabling tests from workstation to cluster scale. Each dataset includes:

- Raw power and timing logs at the kernel and pipeline level, together with energy metrics.
- Ground-truth dirty image to compare algorithmic quality metrics.
- Configuration templates for CPU and GPU runs.

6 Benchmark Evaluation and Results

This section benchmarks the proposed SKA imaging workloads and datasets using SKA-Low configurations to demonstrate the practical impact of our co-design methodology. We present the experimental setup used to obtain reproducible measurements of a subset of the proposed metrics for system-level performance and energy efficiency, sustainability, and economy. We then evaluate heterogeneous WSClean+IDG deployments and analyse the weak scaling behaviour of CPU-only execution. Assuming we were to run identical workloads at the two SKA SDP locations, we quantify how site-specific carbon intensity and electricity prices shape cost and carbon efficiency. Finally, we use PREESM to explore the co-design space for performance–energy–utilization trade-offs. This demonstrates how the proposed methodology can aid in identifying Pareto-optimal operating regions for SKA-scale imaging pipelines.

6.1 Experimental Setup

Benchmarks were executed on a Lenovo ThinkSystem SR675 V3 node of the Green500 KUMA cluster [26], equipped with dual AMD EPYC 9334 CPUs, 371 GB RAM, 6.4 TB NVMe storage, and four NVIDIA H100 GPUs (94 GB). All runs used exclusive node access, with tests using 16 CPU cores, a single H100 GPU and a quarter (92.2 GB) of the full RAM (Slurm configuration limits the memory per CPU core to 5900 MB).

The server cost was obtained by configuring a system with comparable specifications, resulting in 29 875.39 USD [17]. Embodied hardware emissions were estimated by combining the emissions reported by NVIDIA for the H100 GPU (175.944 tCO₂e [20]) with the emissions of the remaining system components modeled using Boavizta’s Datavizta tool [5], yielding a total embodied emission of 512.519 tCO₂e. The latter assumes a Genoa-class CPU architecture, Samsung memory modules, and a Micron SSD. We assume that the CAPEX is amortized over a six-year lifetime.

The data were processed using WSClean [21] using IDG [35] gridded GPU mode. For each of the 16 datasets we produced images with fixed FoV but varying image sizes of 4096², 8192², 16 384² and

32 768² pixels, i.e. with pixel scales of respectively 17.578, 8.789, 4.394 and 2.197 arcsec. For each of the $25 \times 4 = 100$ runs, the data was processed twice in the following sequence: warmup, 120 s pause, run, 120 s pause. The warmup run is not monitored but GPU CUDA kernels of IDG are being compiled while the run is monitored and uses the pre-compiled GPU kernels from warmup stage. The 120 s pause before the monitored run allows the hardware to settle down. Power measurements were recorded using node-level PDUs, which provided a 1 s power average sampled every 5 s. The PDU measurements were cross-validated with software monitors (RAPL, NVML), using the PMT library wrapper [7].

6.2 Heterogeneous WSClean+IDG Deployment

WSClean+IDG executes as a heterogeneous pipeline in which the CPU handles visibility batching, metadata preparation, and kernel scheduling, while the GPU performs all IDG gridding and interpolation. This division achieves high throughput only when the CPU can supply work at a rate sufficient to keep the GPU busy.

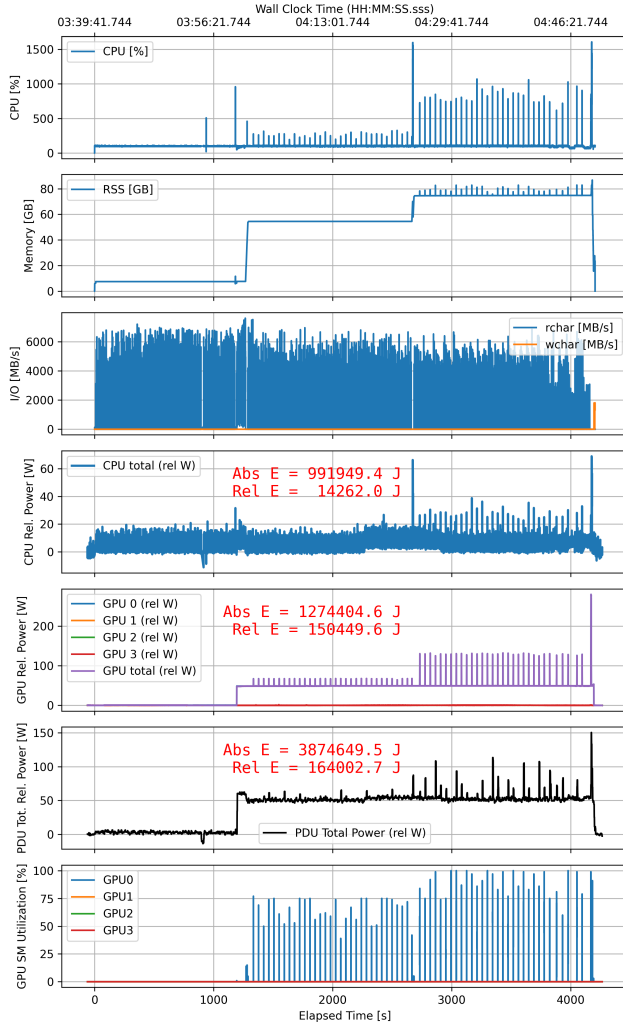


Figure 5: Performance metrics of one run of WSClean+IDG.

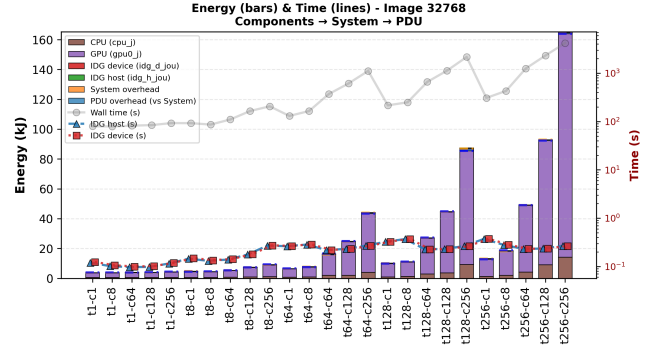


Figure 6: Energy hierarchy for image size 32768² across all ($n_{\text{times}}, n_{\text{chans}}$) configurations. Stacked bars show component-level energy contributions (CPU, GPU, IDG host/device), system overhead, and the corresponding PDU-level measurement. The system total (orange dashed line) and PDU total (blue dashed line) highlight the rack-level overhead above node-level measurements. Execution times (right axis, log scale) include wall time, IDG host time, and IDG device time.

Fig. 5 shows the measurements for one experiment, including CPU utilization, memory footprint and I/O intensity; CPU, GPU and total system power. Power is plotted as a delta over the power measured during idle period. First, the Fig. shows that, most of the time, CPU utilization is limited to one core (100 %), with short peaks of multi-core execution. This reflects the low scalability of the algorithms on the number of CPU cores. Second, GPU power is on average much lower than the rated TDP of the H100, and the utilization of the GPU’s streaming multiprocessors (SMs) is very low, with just short bursts of activity; this shows that either the CPUs are not able to generate work for the GPU promptly, or the GPU is bottlenecked by the access to system memory.

Fig. 6 reveals a clear energy and performance hierarchy for the largest image size (32768²) across all ($n_{\text{times}}, n_{\text{chans}}$) configurations: total consumption is overwhelmingly dominated by the GPU and IDG device, which together account for roughly 60–90% of system energy, while CPU, IDG host, and system-level overheads remain small, flat, and secondary contributors. As workloads scale, GPU energy increases sharply (from ~ 5 –10.kJ for the smallest cases to ~ 165 .kJ for t256-c256). In contrast, CPU and host-side IDG energy stay nearly constant, highlighting the accelerator-driven nature of large-scale imaging. Execution time and energy scale together over almost four orders of magnitude, with the longest runtimes corresponding to the highest energy use, and tightly coupled IDG host/device times indicating a well-balanced heterogeneous execution path. Finally, the comparison across configurations shows that channel-heavy workloads achieve similar throughput with lower wall time and total energy than time-heavy cases, making them systematically more energy-efficient.

We decompose the total energy of the system into *static* and *dynamic* components. Static energy corresponds to the energy consumed by the system in an idle state, including CPUs, GPUs, memory, storage, networking, cooling, and power supply losses. It is estimated as one quarter of the idle power measured at the PDU—reflecting the fraction of node resources used—multiplied by

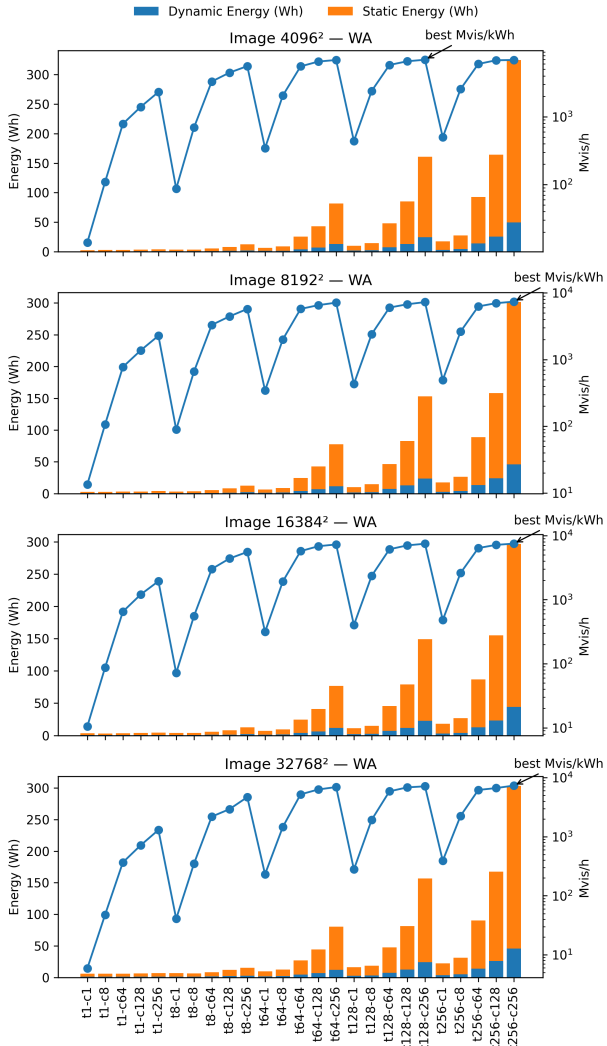


Figure 7: Energy-throughput SKA-Low (WA). Each panel shows a stacked energy breakdown (dynamic + static, in Wh; left axis) alongside throughput (Mvis/h; right axis, log scale), across combinations of timesteps and channels.

the execution time. Dynamic energy is defined as the additional energy consumed during computation relative to this static baseline, and is measured by integrating GPU power and one quarter of CPU power over the execution time. Across all configurations, static energy dominates total consumption, accounting for approximately 80 %–85 % of the total energy. This persistent dominance directly reflects under-utilisation of the hardware, with a large fraction of the system’s available power capacity remaining unused even at the largest problem scales.

We analyze with Fig. 7 how energy and throughput vary across the astroCAMP dataset configurations. As image size and visibility dimensions increase, throughput improves initially but rapidly saturates, while wall time and total energy grow super-linearly. This

behaviour indicates a transition from a compute-efficient regime to a memory- and bandwidth-bound execution regime, in which additional work no longer translates into proportional gains in Mvis/h. Consequently, naïvely scaling imaging parameters increases operational cost and carbon footprint without delivering commensurate scientific throughput, underscoring the need for efficiency-aware configuration selection for SKA-scale deployments.

6.3 Weak CPU-only Scaling of WSClean+IDG

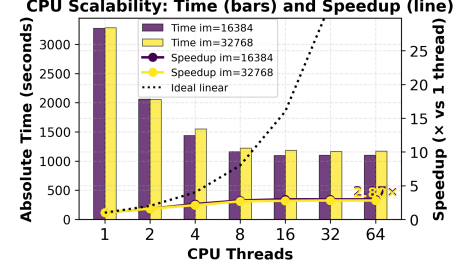


Figure 8: WSClean+IDG on 1–64 CPU threads. Bars show absolute runtime, solid line shows speedup relative to 1 thread, and dotted line indicates ideal linear scaling.

Fig. 8 shows the weak-scaling behaviour of WSClean+IDG across 1–64 CPU threads. Consistent with previous findings [21], performance improves when moving from 1 to 4 threads, but scaling rapidly degrades thereafter. Beyond 8 threads, additional cores yield diminishing returns, and total runtime even increases slightly due to contention on shared resources. The maximum observed speedup is only **2.87 \times at 64 threads**, far from the ideal linear trend. This behaviour reflects well-known memory-bandwidth limitations and thread-synchronisation overheads in gridding-heavy imaging pipelines, which prevent efficient exploitation of many-core CPUs.

Relative to ideal scaling, CPU performance at 64 threads deviates by more than **95%**. These results confirm that current software stacks do not scale linearly for SKA-sized workloads on modern CPU servers, underscoring the need for co-designed kernels and dataflows that are explicitly optimised for hierarchical memory systems and modern node/network topologies.

6.4 Location-Dependent Efficiency for SDPs

In Fig. 9, we analyse the carbon and cost breakdown for our largest image size and relate it to performance efficiency at the two SKA SDP locations using site-specific grid carbon intensities and electricity prices. While throughput is identical at both sites, carbon and cost efficiencies diverge due to local grid and pricing conditions. In both locations, operational emissions dominate total carbon (90–95%), reflecting identical hardware and workload characteristics. Despite this, WA achieves higher carbon efficiency ($\text{Mvis}/\text{kgCO}_2$) owing to its lower grid carbon intensity (0.321 vs. 0.672 kg CO_2/kWh), indicating that throughput and workload characteristics, rather than grid intensity alone, primarily govern carbon efficiency.

In contrast, cost efficiency is primarily driven by CAPEX (89–92%). WA’s higher electricity cost (0.27 kWh vs. 0.19 kWh in WA) results in slightly lower cost efficiency ($\text{Mvis}/\$/$) compared to SA,

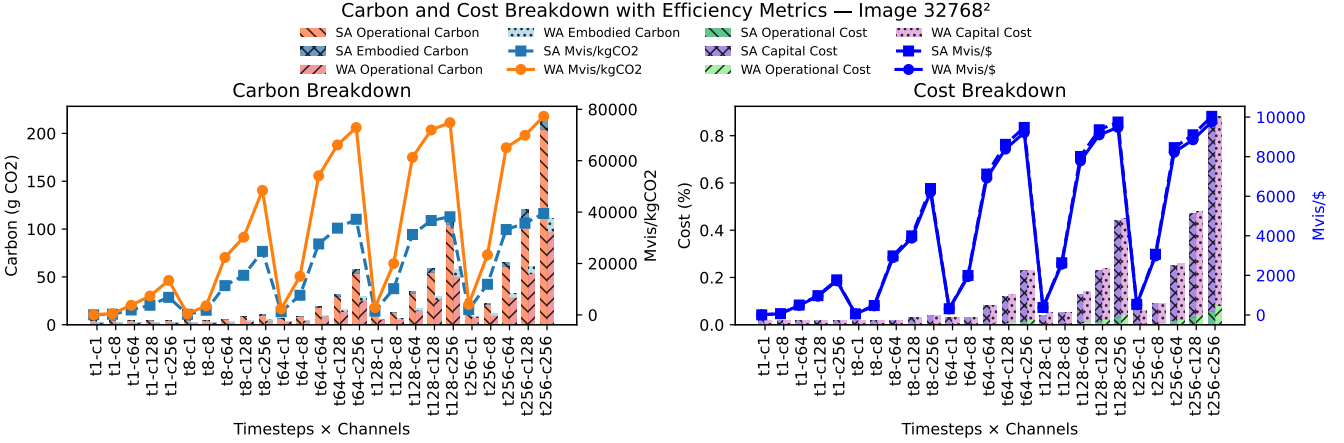


Figure 9: Carbon (left) and cost breakdown (right) with efficiency metrics for the largest image size (32768^2) across all timesteps and channels configurations, comparing SKA-Low (WA) and SKA-Mid (SA).

particularly for larger, longer-running workloads. Across both locations, efficiency improves with increasing timesteps and channels as embodied carbon and capital costs are amortized over greater computational output. This highlights that consolidating workloads into fewer, larger batch jobs can deliver meaningful sustainability and economic benefits, especially in regions with higher electricity prices or carbon intensities.

6.5 Design Space Exploration with PREESM

PREESM [30] is a prime example of a DSE framework to study its extendability. The diversity of metrics, specialized for a scientific field, calls for user made metrics support. The current flow supports many *system* and *hardware platform*-level metrics, and more can be computed from those metrics based on user needs, using an existing model for fast evaluation.

Taking a step back to look at metric implementations, *algorithmic* metrics require the complete execution of the pipeline, with potentially long execution, incompatible with DSE. Future flow will require knowledge of parameters influence on expensive metrics to avoid systematic evaluation [14]. For example, a full execution of a pipeline to evaluate an algorithmic metric is needed when changing quantization parameters, but is not required when changing hardware frequency parameters.

Sustainability and *Economic* metrics are two examples of environmental metrics, based on external information. Those metrics require interaction with external models or databases, bringing a potentially multi-model co-design flow.

We evaluate some of these metrics with PREESM by implementing the simulator, a subset of the DDFacet radio-astronomy pipeline that inverts an artificial sky image into visibilities. We run our designs on a KRIA KR260 SoM board with a 4-core, 1.6 GHz ARM Cortex-A53 processor and an Ultrascale+ FPGA clocked at 150 MHz. We measure each design's resource usage, latency, and energy-to-completion at execution. The energy is obtained by measuring the base consumption of the device at idle and subtracting it from the consumption under load. Fig. 10 summarizes our results. We define

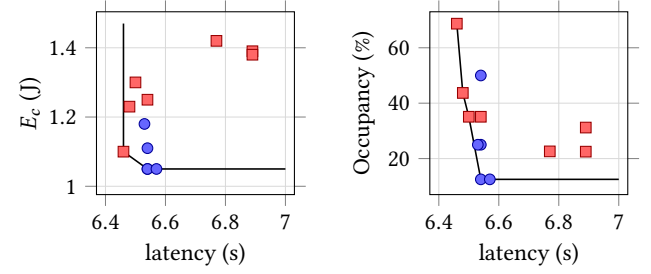


Figure 10: Pareto front generated with PREESM. Square dots represent CPU-FPGA designs; round dots, CPU-only designs.

the occupancy metric as the weighted average between the percentage of cores used and the utilization of three FPGA resources: CLBs, DSPs, and BRAMs : $avg(CPU, avg(CLB, DSP, BRAM))$. This metric aims to measure the proportion of total available computing resources used. The FPGA-mappable computation is the 2-D FFT, split into two 1-D FFTs. The application is run on a 128x128 input image, resulting in a 128x128-point 2-D FFT, and outputs 98k visibilities.

Using PREESM, we can explore the design space and derive the Pareto front shown in Fig. 10. This enables informed design decisions—such as the degree of parallelism and the mapping of tasks to CPU or FPGA—by explicitly trading off target objectives, here latency and energy consumption.

7 Discussion of Benchmark Evaluation

The results presented in the previous section confirm the central hypothesis of this work: that only through algorithm–architecture co-design can radio interferometric imaging achieve sustainable exascale performance. Our preliminary evaluation of WSClean leads to three main conclusions:

- (1) **Scalability limits:** Current imaging algorithms do not exhibit ideal scaling at SKA problem sizes due to memory-bound operations and communication overheads.
- (2) **Co-design imperative:** Achieving sustainable scaling demands joint optimization of algorithms, hardware, and scheduling—targeting reduced-precision arithmetic, data locality, and carbon-aware workload management.

7.1 Why We Need HW–SW Co-Design?

Optimizing the SKA SDP requires the joint consideration of SW and HW design choices, as neither dimension alone is sufficient to fully exploit the available design space across relevant metrics such as energy, carbon emissions, cost, and execution time.

From the SW perspective, profiling of WSClean+IDG reveals severe underutilization of the available HW, with average utilization below 5 %. This underutilization directly translates into wasted static energy, which dominates total energy consumption. By improving SW efficiency and reducing execution time—while assuming the same dynamic energy draw—the total energy consumption can be reduced by up to 81 %. This reduction in energy further translates into a 97 % decrease in carbon emissions and a 32 % reduction in total costs, when accounting for the energy mix and electricity price of Western Australia.

From the HW perspective, architectural exploration can also significantly impact sustainability metrics, particularly when SW efficiency is improved. In the current profiled configuration, dynamic energy accounts for only 15 % of the total energy, limiting the potential impact of HW-level optimizations. However, under the hypothetical scenario of improved HW utilization enabled by SW optimizations, dynamic energy would represent up to 80 % of the total energy consumption. In this regime, architectural improvements—such as energy-efficient FPGA designs—become substantially more impactful. Specifically, a reduction in dynamic energy translates directly into a reduction in operational energy consumption, which corresponds to approximately 78 % of the total carbon emissions and 25 % of the total costs.

This analysis demonstrates that SW and HW optimizations are inherently interdependent. SW-only approaches are constrained by inefficient HW utilization, while HW-only optimizations that target energy efficiency may have limited impact when dynamic energy is a small fraction of total energy. Effective optimization of sustainability metrics therefore requires a holistic HW–SW co-design approach, in which both dimensions are co-optimized to unlock their full potential.

7.2 Community Challenge: How Much Quality can we Trade off for Efficiency?

SKA documents define high-level goals—e.g. 1 % astrometry, spectral dynamic ranges of 10^5 – 10^4 —but not survey-level tolerances on flux accuracy, completeness, PSF residuals, polarisation purity, or spectral-line fidelity. Without such thresholds, the co-design community cannot determine how much approximation (e.g., reduced precision, coarse w -stacking) is scientifically acceptable.

Open Challenge for the SKA Community

For each SKA Key Science Programme—Cosmic Dawn/EoR, Galaxy Evolution and Cosmology, Cosmic Magnetism, and Time-Domain Astrophysics—define quantitative application-level quality metrics and tolerances. Examples include PSNR/SSIM, flux-scale accuracy, astrometric precision, polarisation purity, RM recovery error, spectral-line fidelity, time-series accuracy, and transient completeness. Tolerances must be precise enough to guide hardware–software co-design (precision choices, approximations, accelerators) while ensuring validity for:

- 21 cm EoR power spectra and tomographic cubes,
- all-sky continuum and deep extragalactic surveys,
- RM Grid measurements of cosmic magnetism,
- high-cadence transient and pulsar timing searches.

As SKA power and cost envelopes are fixed years in advance, the central question becomes: *Which combinations of algorithmic parameters and hardware choices maximise performance and energy efficiency without violating scientific fidelity?* Answering this requires cross-layer metrics connecting runtime, energy, carbon, utilisation, and image quality. But the community still lacks programme-level tolerances for key cosmological surveys [4].

8 Conclusions

This paper introduced an open benchmarking and co-design framework for sustainable, reproducible, and energy-efficient radio interferometry imaging at exascale. By coupling representative datasets with unified performance, energy, and carbon metrics, the framework provides a common ground for evaluating algorithms and architectures across heterogeneous platforms. Preliminary results confirm that existing imaging codes do not scale efficiently to SKA-class workloads and that energy and carbon constraints must drive future design choices. The proposed methodology promotes transparent, carbon-aware design-space exploration and establishes benchmarks as shared instruments for scientific accountability. In advancing co-design as both a technical and ethical imperative, this work contributes to building trust in high-performance computing and to reducing the environmental footprint of data-intensive science. We conclude with a community call to: (1) establish science-driven imaging-quality tolerances, (2) expand benchmark datasets, (3) develop reference submissions for current and emerging imaging pipelines, and (4) build an open, MLPerf-style [12, 24] submission and validation process for the SKA era.

9 Acknowledgments

This research was funded, in whole or in part, by the Agence National de la Recherche grant agreements ANR-23-CE46-0010 and ANR-22-EXNU-0004, and the Swiss National Science Foundation grant no. 200021E_220194: “Sustainable and Energy Aware Methods for SKA (SEAMS)”. A CC BY license is applied to the AAM resulting from this submission, in accordance with the open access conditions of the grant. The authors thank the EPFL EcoCloud center, in particular Dr. Xavier Ouvrard, for providing access to its infrastructure for monitoring energy consumption in servers.

References

- [1] Electricity maps. <https://app.electricitymaps.com/>, 2025. Accessed: November 2025.
- [2] ÁLVAREZ, R. R., CONSTANTINESCU, D.-A., PEÓN-QUIRÓS, M., AND ATIENZA, D. Ceo-dc: Driving decarbonization in hpc data centers with actionable insights. *arXiv preprint arXiv:2507.08923* (2025).
- [3] AUJOUX, C., KOTERA, K., AND BLANCHARD, O. Estimating the carbon footprint of the grand project: a multi-decade astrophysics experiment. *Astroparticle Physics* 131 (2021), 102587.
- [4] BACON, D. J., BATTYE, R. A., BULL, P., CAMERA, S., FERREIRA, P. G., HARRISON, I., PARKINSON, D., POURTSIDOU, A., SANTOS, M. G., WOLZ, L., ET AL. Cosmology with phase 1 of the square kilometre array red book 2018: technical specifications and performance forecasts. *Publications of the Astronomical Society of Australia* 37 (2020), e007.
- [5] BOAVIZTA. Datavizta: Environmental Impact Modelling Tool. <https://datavizta.boavizta.org/>, 2024. Accessed: December 2025.
- [6] BROEKEMA, P. C., VAN NIEUWPOORT, R. V., AND BAL, H. E. The square kilometre array science data processor: Preliminary compute platform design. *Journal of Instrumentation* 10, 07 (2015), C07004.
- [7] CORDA, S., VEENBOER, B., AND TOLLEY, E. Pmt: Power measurement toolkit. In *2022 IEEE/ACM International Workshop on HPC User Support Tools (HUST)* (2022), IEEE, pp. 44–47.
- [8] CORDA, S., VEENBOER, B., AND VAN NIEUWPOORT, R. Reduced-precision acceleration of radio-astronomical imaging on reconfigurable hardware. *IEEE Access* 10 (2022), 104780–104795.
- [9] CORNWELL, T. J., GOLAP, K., AND BHATNAGAR, S. The noncoplanar baselines effect in radio interferometry: The w-projection algorithm. *IEEE Journal of Selected Topics in Signal Processing* 2, 5 (2008), 647–657.
- [10] DEWDNEY, P. E., HALL, P. J., SCHILIZZI, R. T., AND LAZIO, T. J. W. The square kilometre array. *Proceedings of the IEEE* 97, 8 (2009), 1482–1496.
- [11] DOS SANTOS ILHA, G., BOIX, M., KNÖLSEDER, J., GARNIER, P., MONTASTRUC, L., JEAN, P., PARESCHI, G., STEINER, A., AND TOUSSANE, F. Assessment of the environmental impacts of the cherenkov telescope array mid-sized telescope. *Nature Astronomy* 8, 11 (2024), 1468–1477.
- [12] FARRELL, S., EMANI, M., BALMA, J., DRESCHER, L., DROZD, A., FINK, A., FOX, G., KANTER, D., KURTH, T., MATTSON, P., ET AL. MpertTM hpc: A holistic benchmark suite for scientific machine learning on hpc systems. In *2021 IEEE/ACM Workshop on Machine Learning in High Performance Computing Environments (MLHPC)* (2021), IEEE, pp. 33–45.
- [13] FU, V., BENAZOUZ, M., ZAOURAR, L., AND MUNIER-KORDON, A. High-performance computing architecture exploration with stage-enhanced bayesian optimization. In *2025 62nd ACM/IEEE Design Automation Conference (DAC)* (2025), IEEE, pp. 1–7.
- [14] HONORAT, A., BOURGOIN, T., MIOMANDRE, H., DESNOS, K., MENARD, D., AND NEZAN, J.-F. Influence of Dataflow Graph Moldable Parameters on Optimization Criteria. In *DASIP 2022 - Workshop on Design and Architectures for Signal and Image Processing* (Budapest, Hungary, June 2022), vol. 13425 of *Lecture Notes in Computer Science*, Springer International Publishing, pp. 83–95.
- [15] HURLEY-WALKER, N., CALLINGHAM, J. R., HANCOCK, P. J., FRANZEN, T. M. O., HINDSON, L., KAPIŃSKA, A. D., MORGAN, J., OFFRINGA, A. R., WAYTH, R. B., WU, C., ZHENG, Q., MURPHY, T., BELL, M. E., DWARAKANATH, K. S., FOR, B., GAENSLER, B. M., JOHNSTON-HOLLITT, M., LENC, E., PROCOPIO, P., STAVELEY-SMITH, L., EKERS, R., BOWMAN, J. D., BRIGGS, F., CAPPALLO, R. J., DESHPANDE, A. A., GREENHILL, L., HAZELTON, B. J., KAPLAN, D. L., LONSDALE, C. J., MCWHIRTER, S. R., MITCHELL, D. A., MORALES, M. F., MORGAN, E., OBEROI, D., ORD, S. M., PRABU, T., SHANKAR, N. U., SRIVANI, K. S., SUBRAHMANYAN, R., TINGAY, S. J., WEBSTER, R. L., WILLIAMS, A., AND WILLIAMS, C. L. GaLactic and Extragalactic All-sky Murchison Widefield Array (GLEAM) survey - I. A low-frequency extragalactic catalogue. *MNRAS* 464, 1 (Jan 2017), 1146–1167.
- [16] KNÖLSEDER, J., BRAU-NOGUÉ, S., CORIAT, M., GARNIER, P., HUGHES, A., MARTIN, P., AND TIBALDO, L. Estimate of the carbon footprint of astronomical research infrastructures. *Nature Astronomy* 6, 4 (2022), 503–513.
- [17] LENOVO. ThinkSystem SR675 V3 Server. <https://www.lenovo.com/us/en/p/servers-storage/servers/inferencing/thinksystem-sr675-v3/len21ts0007>, 2024. Accessed: December 2025.
- [18] MONNIER, N., RAFFIN, E., TASSE, C., NEZAN, J.-F., AND SMIRNOV, O. M. Parallelisation of the wide-band wide-field spectral deconvolution framework ddfacet on distributed memory hpc system. In *ADASS* (2020).
- [19] MORT, B. J., DULWICH, F., SALVINI, S., ADAMI, K. Z., AND JONES, M. E. Oskar: Simulating digital beamforming for the ska aperture array. In *2010 IEEE International Symposium on Phased Array Systems and Technology* (2010), pp. 690–694.
- [20] NVIDIA. HGX H100 Product Carbon Footprint Summary. <https://images.nvidia.com/aem-dam/Solutions/documents/HGX-H100-PCF-Summary.pdf>, 2023. Accessed: December 2025.
- [21] OFFRINGA, A. R., MCKINLEY, B., HURLEY-WALKER, N., BRIGGS, F. H., WAYTH, R. B., AND KAPLAN, D. L. Wsclean: an implementation of a fast, generic wide-field imager for radio astronomy. *Monthly Notices of the Royal Astronomical Society* 444, 1 (2014), 606–619.
- [22] PORTEGIES ZWART, S. The ecological impact of high-performance computing in astrophysics. *Nature Astronomy* 4, 9 (2020), 819–822.
- [23] PRATLEY, L., JOHNSTON-HOLLITT, M., AND McEWEN, J. D. A fast and exact w-stacking and w-projection hybrid algorithm for wide-field interferometric imaging. *The Astrophysical Journal* 874, 2 (2019), 174.
- [24] REDDI, V. J., CHENG, C., KANTER, D., MATTSON, P., SCHMUELLING, G., WU, C.-J., ANDERSON, B., BREUGHE, M., CHARLEBOIS, M., CHOU, W., ET AL. Mpert inference benchmark. In *2020 ACM/IEEE 47th Annual International Symposium on Computer Architecture (ISCA)* (2020), IEEE, pp. 446–459.
- [25] SARKAR, R., AND HAO, C. LightningSim: Fast and Accurate Trace-Based Simulation for High-Level Synthesis. In *International Symposium on Field-Programmable Custom Computing Machines (FCCM)* (May 2023), pp. 1–11.
- [26] SCITAS, E. Kuma cluster. <https://scitas-doc.epfl.ch/supercomputers/kuma/>. Accessed: 2025-11-27.
- [27] SEAMS PROJECT. astroCAMP: A Framework for Cross-Layer Co-Design of Radio Astronomy Imaging Pipelines. <https://github.com/SEAMS-Project/astroCAMP>, 2025. Accessed: 2025-12-13.
- [28] SKAO COMMUNICATIONS. Environmental footprint | skao, 2024. Details SKAO's goals to measure, monitor, and minimise environmental impact and use renewable energy.
- [29] SKAO COMMUNICATIONS. Sustainability at the skao, 2024. Outlines SKAO's commitment to sustainability and alignment with UN SDGs.
- [30] SURIANO, L., RODRIGUEZ, A., DESNOS, K., PELCAT, M., AND DE LA TORRE, E. Analysis of a heterogeneous multi-core, multi-hw-accelerator-based system designed using preesim and sdsoc. In *2017 12th International Symposium on Reconfigurable Communication-centric Systems-on-Chip (ReCoSoC)* (2017), pp. 1–7.
- [31] TASSE, C., HUGO, B., MIRMONT, M., SMIRNOV, O., ATEMKENG, M., BESTER, L., HARDCASTLE, M., LAKHOO, R., PERKINS, S., AND SHIMWELL, T. Ddfacet: Facet-based radio imaging package. *Astrophysics Source Code Library* (2023), ascl-2305.
- [32] TOLLEY, E., FRASCH, S., ORLIAC, E., KRISHNA, S., BIANCO, M., KASHANI, S., HURLEY, P., SIMEONI, M., AND KNEIB, J.-P. Bipp: An efficient hpc implementation of the bluebild algorithm for radio astronomy. *Astronomy and Computing* 51 (2025), 100920.
- [33] TOP500.ORG. Green500 list – november 2025. <https://top500.org/lists/green500/2025/11/>. Accessed: December 2025.
- [34] VAN DER TOL, S., VEENBOER, B., AND OFFRINGA, A. R. Image domain gridding: a fast method for convolutional resampling of visibilities. *Astronomy & Astrophysics* 616 (2018), A27.
- [35] VAN DER TOL, S., VEENBOER, B., AND OFFRINGA, A. R. Image domain gridding: A fast method for convolutional resampling of visibilities. *Astronomy & Astrophysics* 616 (2018), A27.
- [36] VEENBOER, B., AND ROMEIN, J. W. Radio-astronomical imaging on graphics processors. *Astronomy and Computing* 32 (2020), 100386.
- [37] WU, S., XIE, Y., WANG, F., XU, Y., DENG, H., MEI, Y., LÜ, Y.-H. C., HODOSÁN, G., AND ZHU, Y. Performance comparison of source finders in imaging quality assessment for ska1-low. *The Astronomical Journal* 170, 6 (2025), 308.
- [38] ZAOURAR, L., CHILLET, A., AND PHILIPPE, J.-M. A-deca: an automated design space exploration approach for computing architectures to develop efficient high-performance many-core processors. In *2023 26th Euromicro Conference on Digital System Design (DSD)* (2023), IEEE, pp. 756–763.